Supplement of Geosci. Model Dev., 17, 8093–8114, 2024
https://doi.org/10.5194/gmd-17-8093-2024-supplement

Geoscientific Model Development
Open Access
EGU

Supplement of

An updated parameterization of the unstable atmospheric surface layer in the Weather Research and Forecasting (WRF) modeling system

Prabhakar Namdev et al.

Correspondence to: Prabhakar Namdev (prabhakarnmdv587@gmail.com)

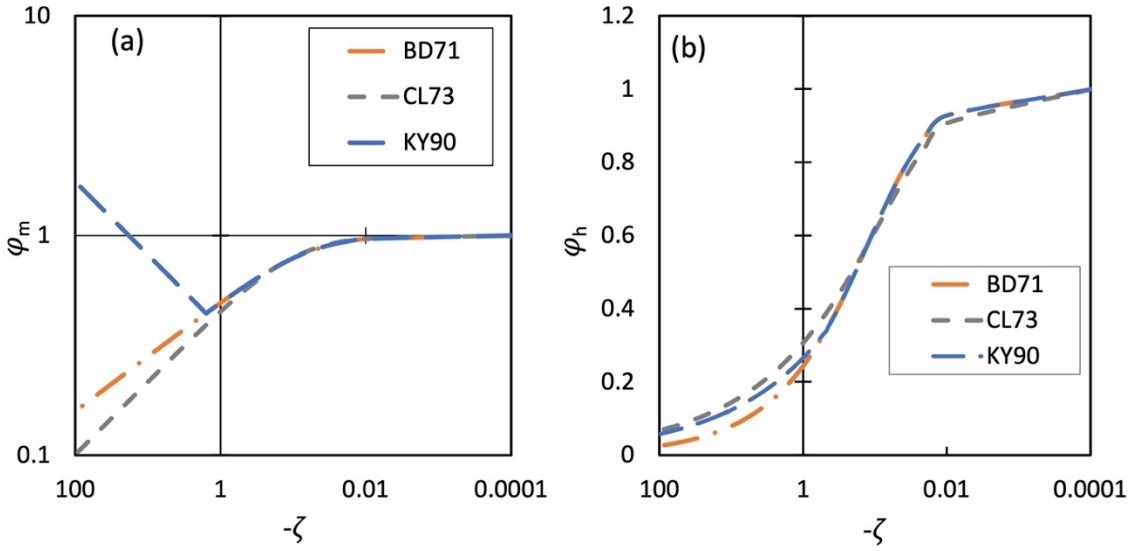

Figure S1. Variation of different functional forms of φ_m and φ_h with respect to $-\boldsymbol{\zeta}$ utilized in this study based on the different classes.

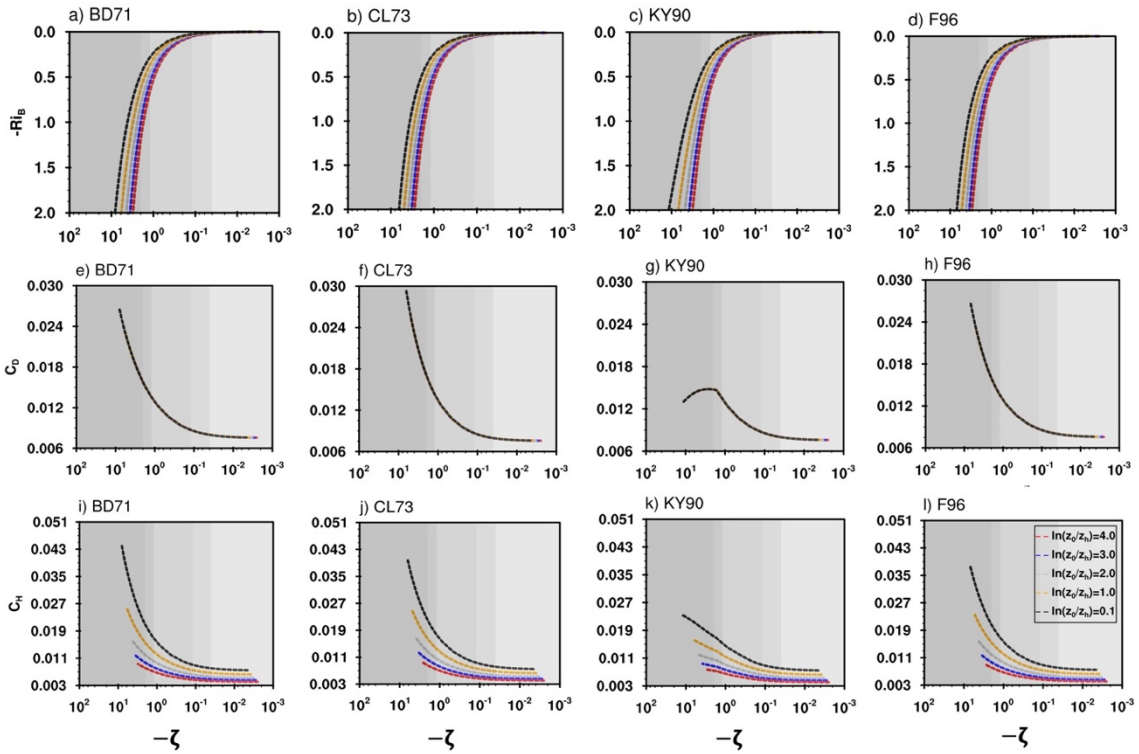

Figure S2. Variation of ζ with Ri_B (upper panel), C_D (middle panel) and C_H (lower panel) with ζ calculated from bulk flux algorithm (offline simulation) for different functional forms of similarity functions corresponding to BD71, CL73, KY90, and F96 forms for different values of z_h for the case when $z_0 = 0.1$ m. The background color corresponds to different sublayers in convective conditions (Kader and Yaglom 1990), from the dynamic sublayer ($0 \geq \zeta > -0.04$; light grey) to the free convective sublayer ($\zeta < -2$; dark grey).

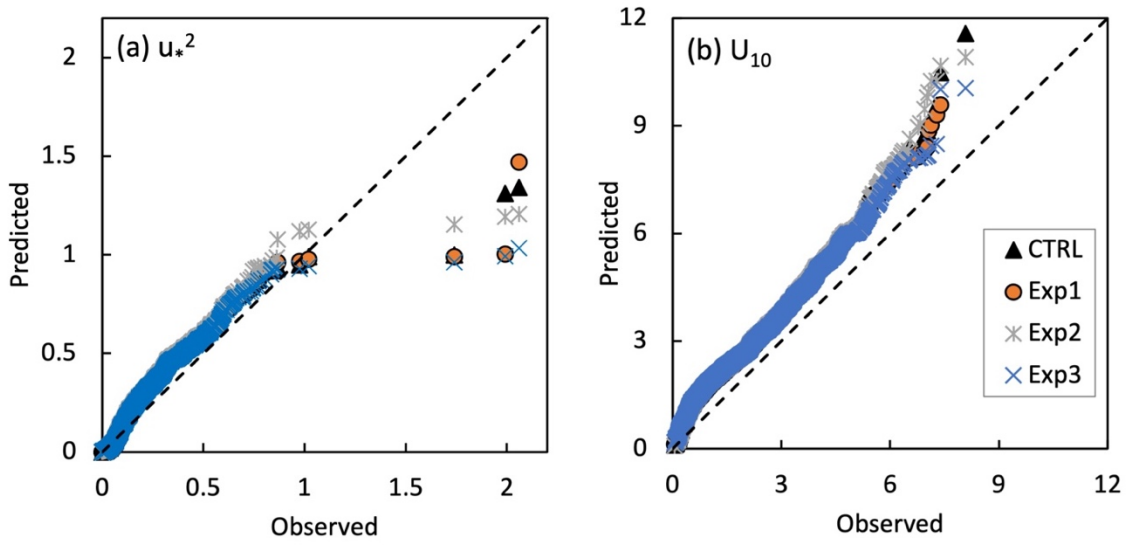

Figure S3. Q-Q plot for model simulated (a) $\boldsymbol{u_*^2}$, and (b) U_{10} from different experiments and CTRL simulation with respect to the observational data derived from the flux tower at Ranchi (India) during MAM season (2009).

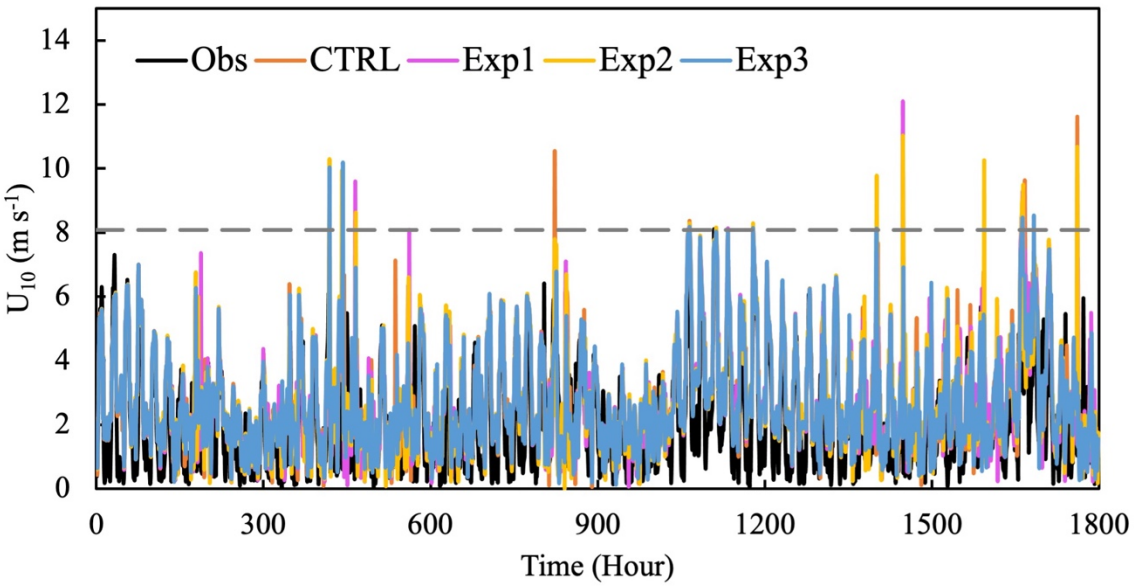

Figure S4. Time variation of 10-m wind speed predicted from different similarity functions in the surface layer scheme of WRF model. The maximum value of wind speed in observational data is shown by dotted grey line.

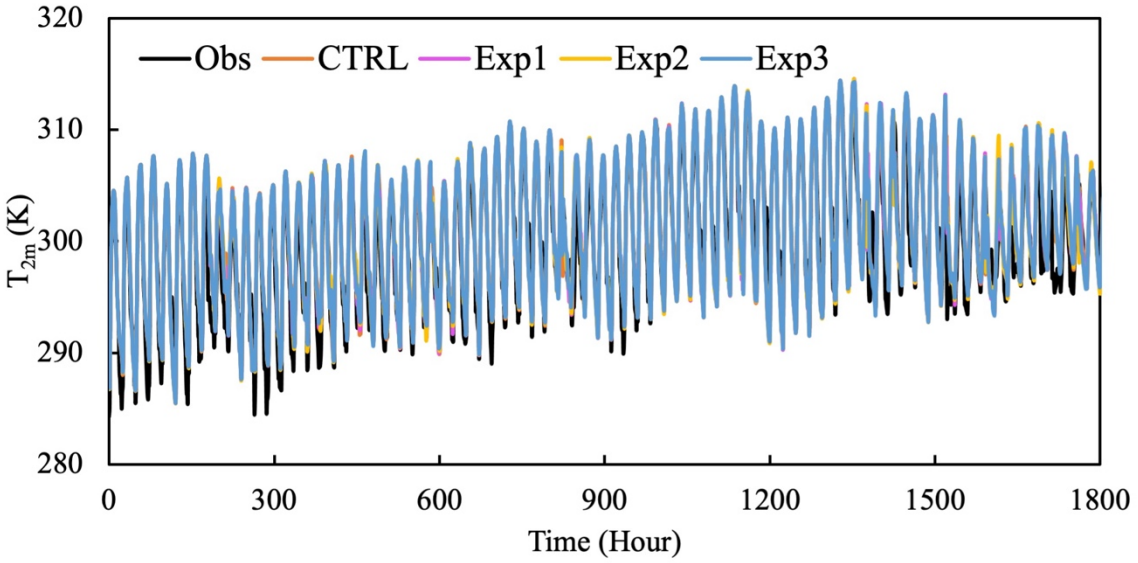

Figure S5. Time variation of 2-m temperature predicted from different similarity functions in the surface layer scheme of WRF model.

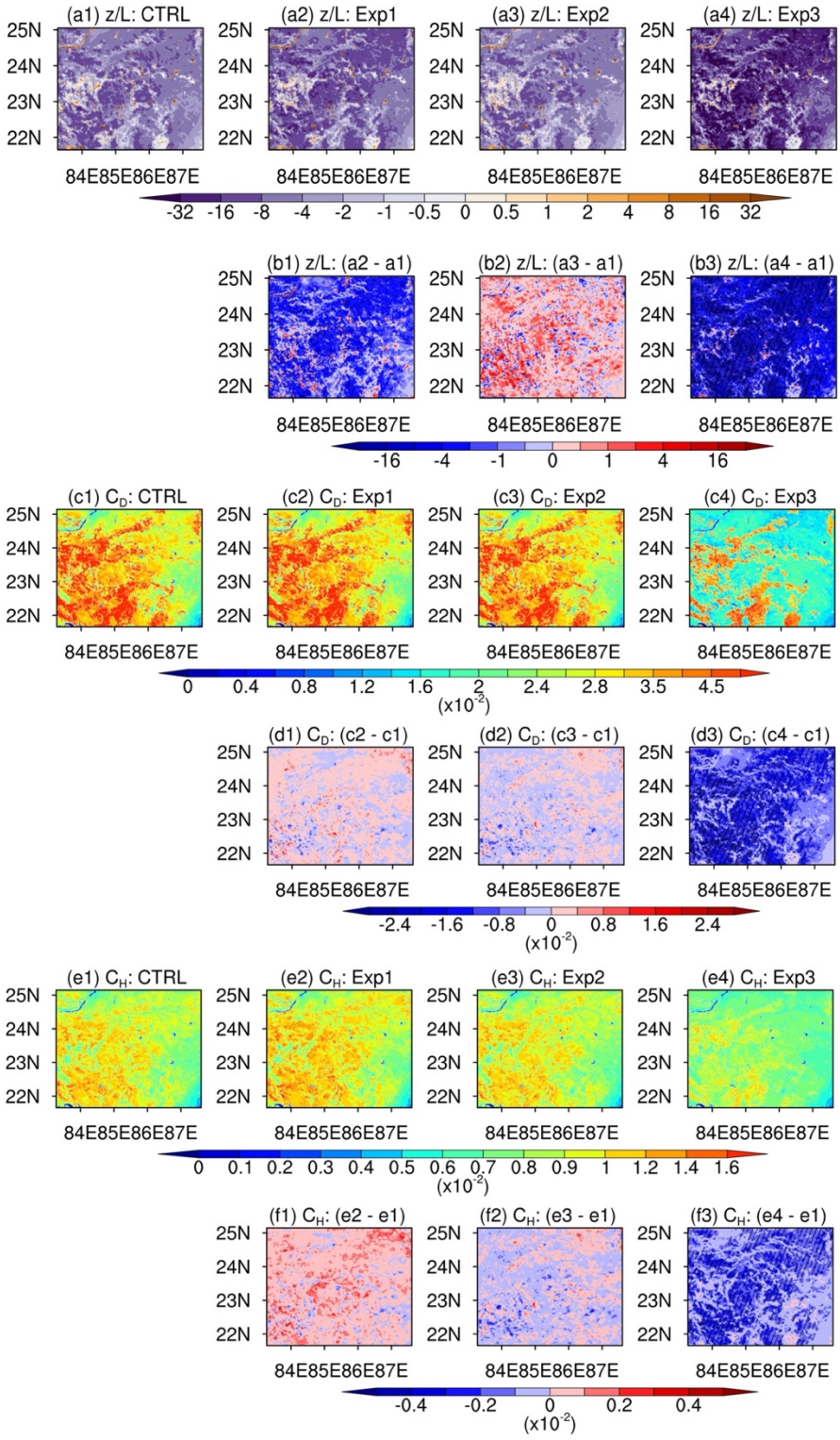

Figure S6: Mean spatial distribution of model simulated ζ (1st row), C_D (2nd row) and C_H (3rd row) from different experiments and their differences with respect to CTRL simulation averaged during strong unstable conditions (hours during daytime in which $\boldsymbol{\zeta}$ is smaller than $\mathbf{-10}$) for whole simulation period. Hatched regions show significant differences at 95% confidence level in experiments with respect to CTRL simulation.

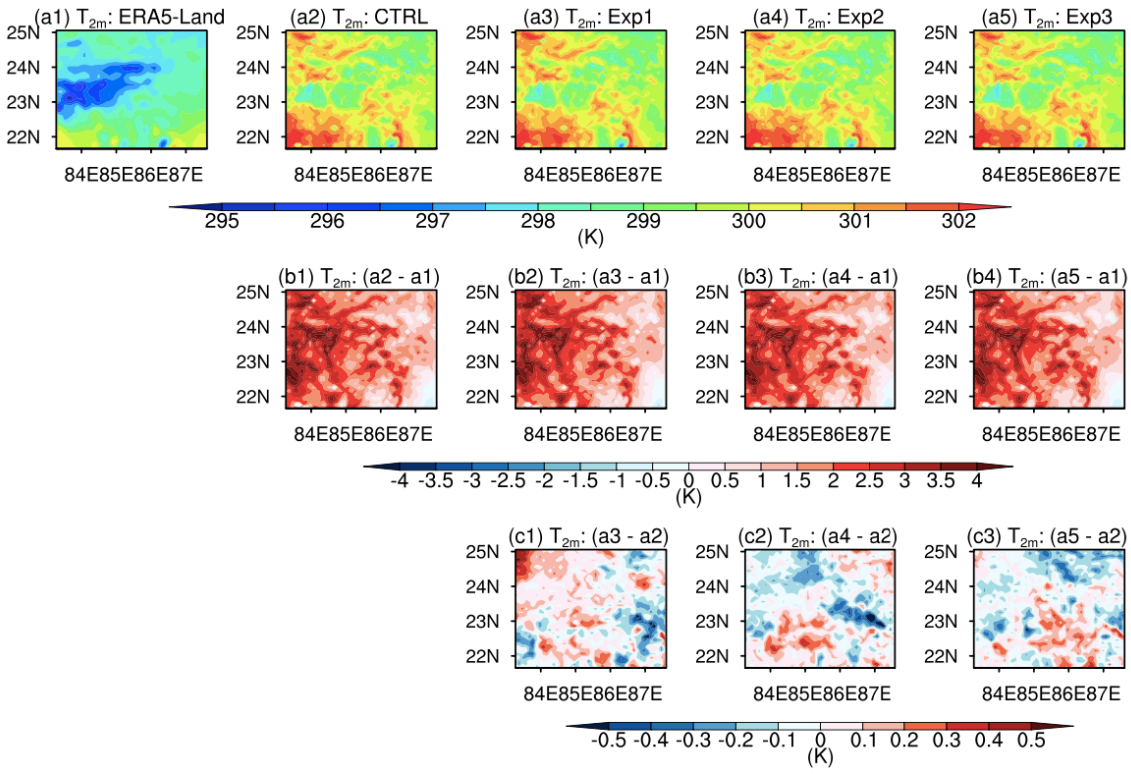

Figure S7: Mean spatial distribution of T_{2m} from ERA5 land reanalysis (a1) and simulated using different experiments (a2-a5) and their differences with respect to ERA5 land reanalysis data (b1-b4) averaged during strong unstable regime (hours during daytime in which $\boldsymbol{\zeta}$ is smaller than $\mathbf{-10}$) for whole simulation period. The differences between different experiments and CTRL simulation are shown in last row (c1-3).

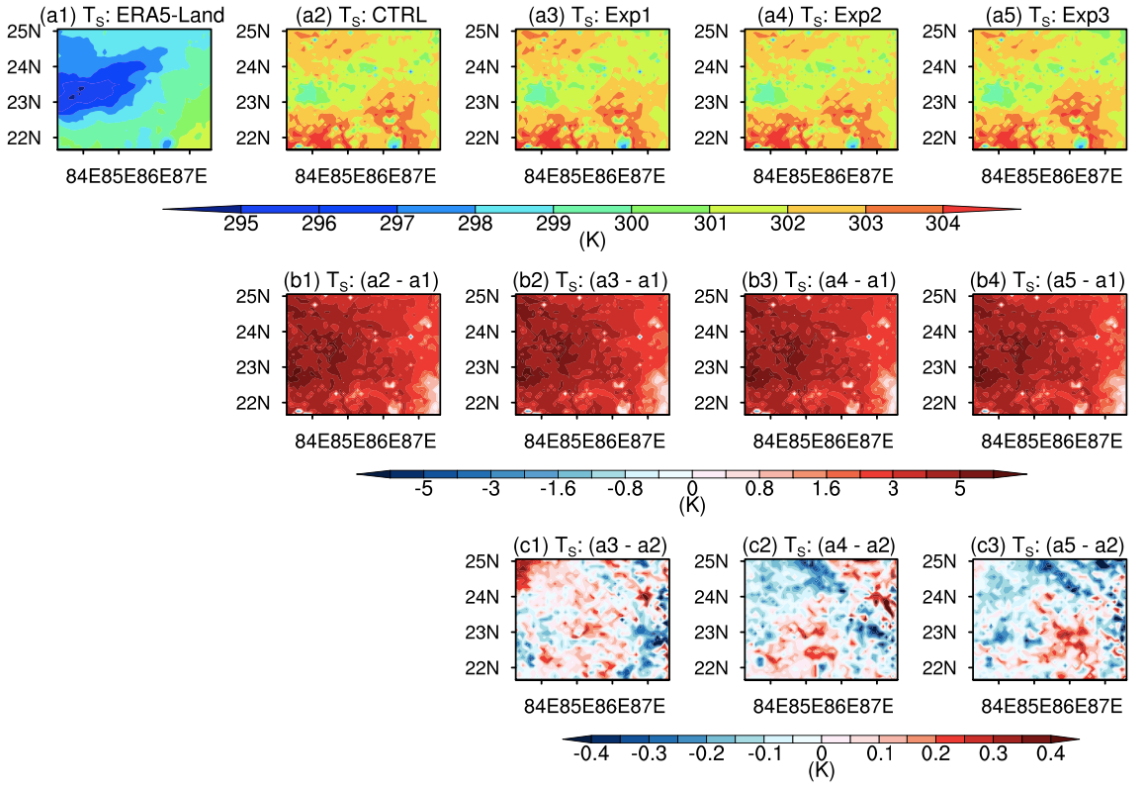

Figure S8: Same as Figure S7 but for T_S.

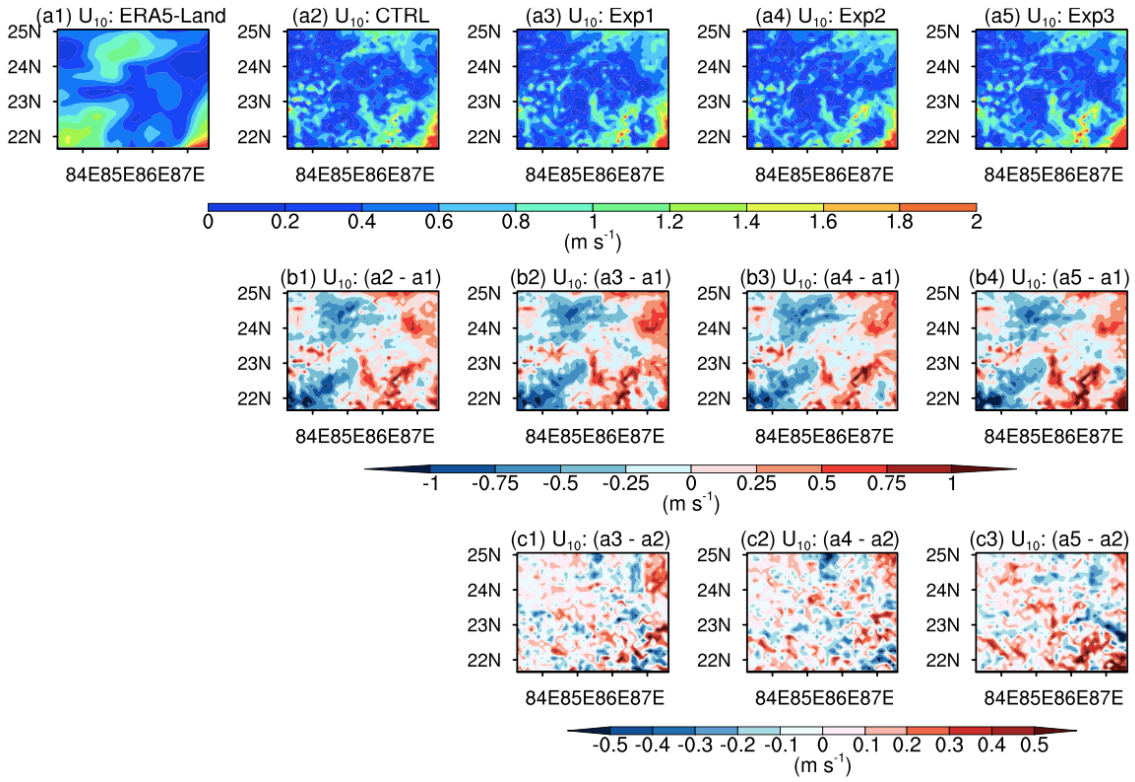

Figure S9: Same as Figure S7 but for U_{10}.

MAM		Bias (%)	RMSE	PCC
SHF (W m^{-2})	CTRL	7.09	37.37	0.47
	Exp1	7.04	37.42	0.47
	Exp2	7.12	37.44	0.46
	Exp3	7.17	37.42	0.48
LHF (W m^{-2})	CTRL	-33.54	50.70	0.39
	Exp1	-33.54	50.70	0.38
	Exp2	-33.58	50.72	0.39
	Exp3	-33.55	50.71	0.38
T_{2m} (K)	CTRL	0.24	1.26	0.72
	Exp1	0.24	1.26	0.72
	Exp2	0.24	1.26	0.72
	Exp3	0.25	1.27	0.72
T_S (K)	CTRL	0.51	2.75	0.50
	Exp1	0.51	2.76	0.50
	Exp2	0.51	2.76	0.50
	Exp3	0.50	2.75	0.51
U_{10} (m s^{-1})	CTRL	32.28	0.54	0.89
	Exp1	32.12	0.54	0.90
	Exp2	31.18	0.54	0.89
	Exp3	32.06	0.53	0.91

Table S1: Comparison statistics for SHF (W m^{-2}), LHF (W m^{-2}), T_{2m} (K), T_S (K), and U_{10} (m s^{-1}) simulated using different experiments together with CTRL simulation with respect to ERA5 land reanalysis data averaged during daytime for the entire simulation period. The mean bias (%), pattern correlation coefficient (PCC), and root mean square error (RMSE) are shown.